VOL. 11, NO. 1, JANUARY 2016 ISSN 1819-6608
ARPN Journal of Engineering and Applied Sciences

www.arpnjournals.com

FINITE VOLUME ANALYSIS OF PRESSURIZED UNDERFILL ENCAPSULATION PROCESS

Aizat Abas[1], M. H. H. Ishak[1] and M. Z. Abdullah[2]
[1]School of Mechanical Engineering, Universiti Sains Malaysia, Engineering Campus, Nibong Tebal, Penang, Malaysia
[2]School of Aerospace Engineering, Universiti Sains Malaysia, Engineering Campus, Nibong Tebal, Penang, Malaysia

ABSTRACT

This paper studies the effects of pressurized underfill process during chip encapsulation process on a 10 by 10 ball-grid-array (BGA) orientation. Underfill encapsulation play an important role to improve the reliability of flip chip package, yet the conventional capillary underfill (CUF) encapsulation process is subjected to several drawbacks such as extended filling time, incomplete filling and voids formation. To avert this problems relating to fluid flow, pressurized underfill (PUF) is introduced. The filling time, pressure, velocity and flow front propagation are observed during the pressurized filling process. The findings show velocity and pressure buildup at the start of the filling. Moreover, racing effect can observed during the whole filling process due to forced flow.

Keywords: finite volume method, electronic packaging, pressurized encapsulation.

INTRODUCTION

The advent of the semiconductor on integrated circuits (IC) has driven the shift towards optimization of product performance alongside with miniaturization trend. Hence, the use of flip-chip ball grid array (BGA) appears promising with a great number of interconnection pins under limited surface mount. Even so, the miniaturization trends often disclose limitations in the part of the design and manufacturing process [1-3].

The sophisticated and micro-scale sized IC package has brought several challenges and uncertainties to the encapsulation process. In general, the encapsulation of IC components with epoxy molded compound (EMC) prevents physical damage and corrosion due to environmental condition. However, the encapsulated components often encounter defect issues as the results of incomplete filling and voids formation during encapsulation process. The underlying cause of incomplete filling and voids formation usually lies on the velocity and pressure of the flow which the interest of the current study.

The capillary underfill (CUF) encapsulation process is one of the examples of the classical problem in the underfill encapsulation technology; nonetheless, it has significantly improved the reliability of IC package especially the flip-chip BGA [4, 5]. The main challenges of CUF encapsulation include extended filling time, incomplete filling and voids formation. To uplift this problem, the pressurized underfill encapsulation process is introduced [6].

The research work by Zhang and Wong has presented the innovation in flip-chip underfill technology (7). Several improvements have been introduced to overcome the issues associated with CUF, such as pressurized, vacuum-assisted and gravity underfill encapsulation [8, 9]. In the industrial practice, the pressurized underfill (PUF) encapsulation is apparently adopted. The research on PUF encapsulation process is also active.

Experimental observation of encapsulation process is rather restricted since the BGA package is micro-scale in size and can be costly to construct. For that reason, CFD tool has been extensively used to model and simulate the fluid flow of the encapsulation process the simulation approach is believed to enhance the visualization aspect of the process in either 2-D or 3-D [10, 11].

Navier-Stokes formulation

The governing equations according to the Navier-Stokes equation are utilized to simulate the fluid flow of encapsulant material and air using the conservation of mass and momentum. In the encapsulation process, both fluids are assumed to be incompressible and laminar.

Continuity equation

$$\frac{\partial \rho}{\partial t} + +\nabla.(\rho\vec{u}) = 0 \quad (1)$$

Momentum equation

$$\frac{\partial}{\partial t}(\rho\vec{u}) + \nabla.(\rho\vec{u}\vec{u}) = -\nabla P + \nabla.\bar{\bar{\tau}} + \rho\vec{g} (2)$$

In the model, EMC and air are distinguished using multiphase formulation. The volumes of fluids (VOF) for both phases are described using transport equation whilst the distribution of fluid is represented by volume fraction, f within the range of $0 < f < 1$. Generally, $f = 0$ indicate the absence of EMC while $f = 1$ indicate the cell is completely filled with EMC.

VOL. 11, NO. 1, JANUARY 2016 ISSN 1819-6608
ARPN Journal of Engineering and Applied Sciences

www.arpnjournals.com

Transport equation

$$\frac{df}{dt} + \nabla.(\bar{u}f) = 0 \quad (3)$$

where$\vec{u}$ is the fluid velocity vector, ρ is the fluid density, P is the static pressure and $\bar{\bar{\tau}}$ represents the stress tensor.

Rheological formulation

In this project, the rheological constitutive relation to describe the pressurized underfill (PUF) on 10 by 10 BGA case is modeled using Castro-Macosko rheology model. This model is found to be more stable and reliable in describing the encapsulant since it takes into account the curing effect throughout the encapsulation process.

Castro-Macosko model

$$\Phi = \eta\dot{\gamma}^2 + \dot{\alpha}\Delta H \quad (4)$$

$$\eta(t,\dot{\gamma}) = \frac{\eta_o(T)}{1+\left(\frac{\eta_o(T)\dot{\gamma}}{\tau^*}\right)^{1-n}}\left(\frac{\alpha_g}{\alpha_g-\alpha}\right)^{C_1+C_2\alpha} \quad (5)$$

$$\eta_o(T) = B^{(T_b/T)} \quad (6)$$

Schematic diagram of BGA

A 3D fluid flow simulation through ball grid array is described. Figure-1 depicts the schematic diagram of underfill process for the flow. The BGA will consist of square array of spherical solder balls across the surface attached to a printed circuit board (PCB).

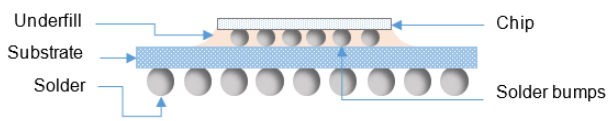

Figure-1. Schematic diagram of flip-chip BGA package.

During manufacturing process, BGA solder balls are spaced evenly to prevent bridging or sticking problems. The advantage of BGA package is apparent since it has better performance for pressurized or high velocity flow. The BGA uses the underside of the package for the connection in which the pins are arranged in grid pattern as depicted in Figure-2. Balls of solder are used for replacement of the pins to provide the connectivity. BGA package also offers lower thermal resistance within silicon chip allowing more heat to be conducted out of the device.

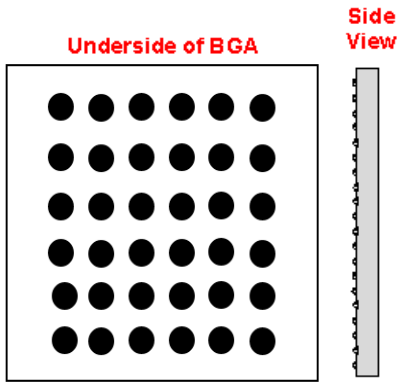

Figure-2. Ball Grid Array (BGA) package diagram.

Figure-3 shows the underfill process involving the dispensing process of controlling the amount of material into the gap between the chip and substrate. The underfill encapsulation of ball grid array (BGA) is important in protecting and increasing reliability of the electronic packaging (EP) as it can reduce the global thermal expansion, stresses and strains between the silicon chip and substrate. The gap between the chip and silicon has to be completely filled with underfill material (underfill material flow correctly) in order to protect life of the chip assembly (12).

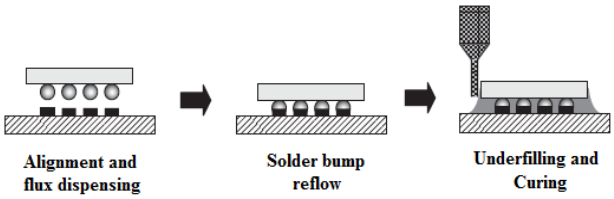

Figure-3. Underfill process flow.

Numerical simulation

The 3-D geometrical model was developed for a 10 by 10 BGA on a full orientation array. The schematic diagrams of the model are as presented in Figure-2. The dimensions for 10 by 10 BGA model are in accordance to the actual sized BGA as given in Table-1. The encapsulant material used is the epoxy-molded compound (EMC) with properties summarized in Table-2.

Table-1. Dimension of 10 by 10 BGA package.

Parameter	Value
Parallel plates (mm)	10.5(L) x 10.5(W)
Bump diameter (mm)	0.5
Bump pitch (mm)	1.0
Bump height (mm)	0.495

ARPN Journal of Engineering and Applied Sciences

Table-2. EMC encapsulant material properties.

Parameter	Value
Density (g/cm³)	1.843
Specific heat capacity (j/kg-c)	1163
Thermal conductivity (w/m-c	0.8
Molecular weight (kg/kgmol)	44.05358
Standard state enthalpy (j/kgmol)	-1.653202e+08
Reference temperature (c)	24.85001

FVM Boundary condition

The initial and boundary conditions used in the numerical computation are listed as follow:

On wall: $u = v = w = 0;\ \ T = T_{wall};\ \frac{\partial p}{\partial n} = 0$

At inlet:

$P = P_{in}(x, y, z, t);\ \ T = T_{in}$

On flow front:

$$P = P_{atm} - \frac{\sigma}{R} = P_{atm} - \frac{2\sigma \cos\theta}{h}$$

RESULTS AND DISCUSSIONS

Pressure underfill formulation

This section presents the result and discussion on PUF encapsulation on 10 by 10 BGA. The encapsulant is dispensed with the pressure value of 0.5MPa and the curing effect is formulated by Castro-Macosko rheology model.

Table-3. Filling time of PUF encapsulation.

Filling Percentage (%)	20%	40%	60%	80%	100%
Time (s)	10	18	28	35	59
Filling rate (% per s)	2.00	2.20	2.14	2.29	1.69

Figure-4 represents the flow front profile of the 10 by 10 BGA at distinct percentage filling. The racing effect typically occurs in the region between solder bumps. Noticeable delay at the region behind solder bumps can be clearly identified by contemplating on the yellow contour of encapsulant volume fraction. It indicates that only 70% of encapsulant occupying the region. Table-3 pointed out that the average filling rate is 2.06% per second and reached a maximum value of 2.29% per second at 80% of filling. The total filling time of the complete PUF encapsulation process is 59s.

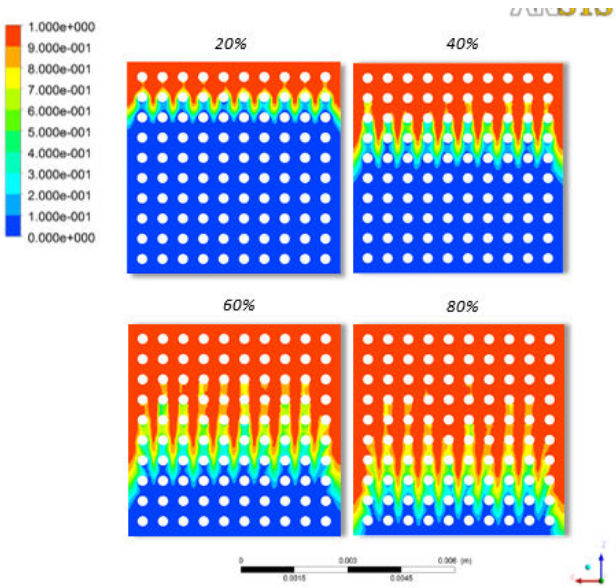

Figure-4. Flow front profile at different percentage filling of PUF encapsulation.

The flow front is driven by a high initial speed that corresponds to the pressure of dispense. In the region between solder bumps, the speed builds up and consequently the racing effect become evident with apparent delay of filling. Subsequently, the filling rate

increases from 40% to 80% of filling to compensate the delay of filling. The racing effect issue in PUF encapsulation may extend to incomplete filling or void formation.

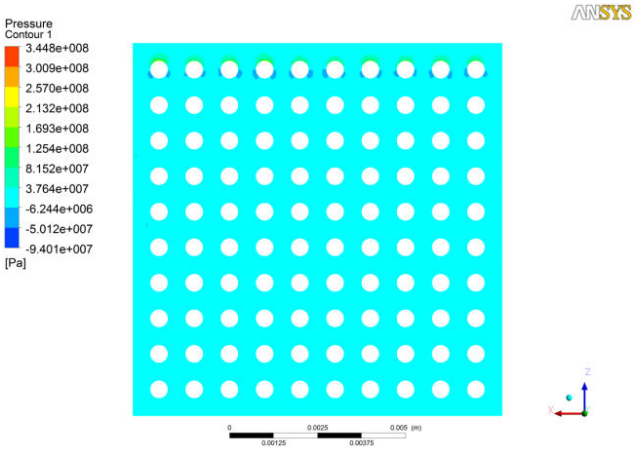

Figure-5. Pressure contour at early stage of filling of PUF encapsulation.

From Figure-6, the pressure near inlet peaked at about 3.4MPa. This value is relatively higher than the dispense pressure at inlet which is only 0.5MPa. Figure 5 illustrates the pressure contour when flow front hits the first row of solder bumps. It can be seen that higher pressure is exerted on the bumps at about 344MPa. Towards the end of filling, the flow front pressure reduces to a maximum value of 0.12MPa as depicted in Figure-7.

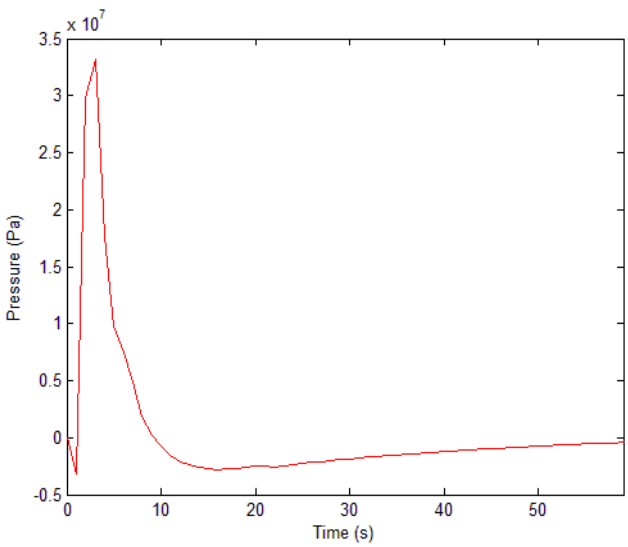

Figure-6. Pressure at point near inlet of PUF encapsulation.

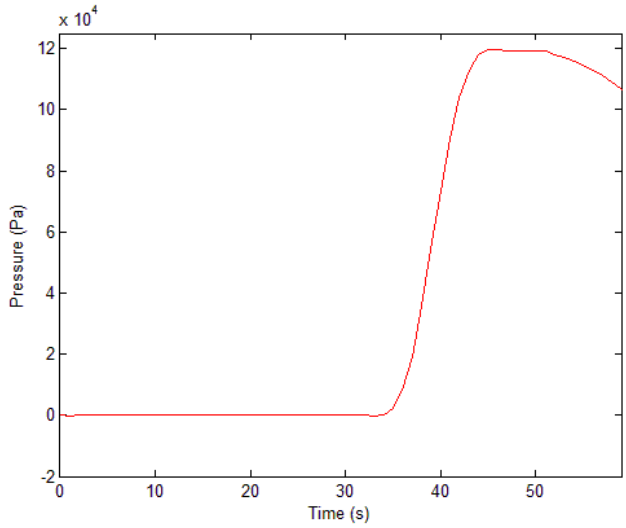

Figure-7. Pressure at point near outlet of PUF encapsulation.

This situation is caused by constant pressure input at the inlet dispenser. The pressure builds up to a relatively high value due to continuous pressurized dispense of encapsulant. During the collision with solder bumps, the flow front pressure increases to overcome the resistance. The end stage of filling shows decline of flow front pressure since it was loss to the resistance of several rows of solder bumps.

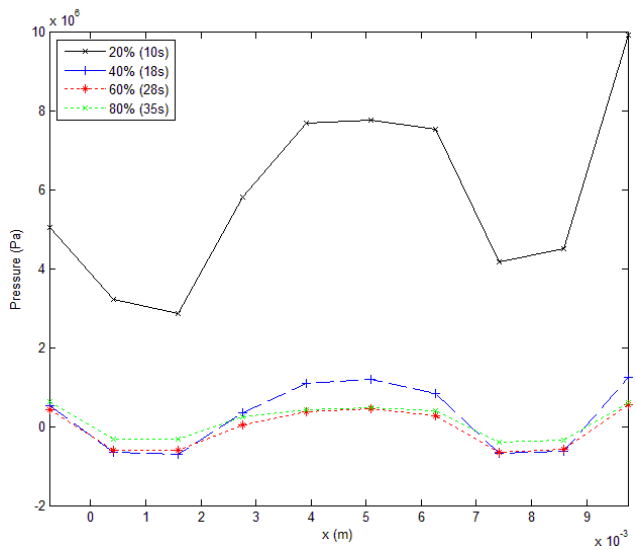

Figure-8. Pressure distribution near inlet at different filling percentage of PUF encapsulation.

Similarly to the preceding discussion, Figure-8 shows the pressure distribution that decline steadily with time. The pressure at 20% of filling is much higher than at the rest of the filling percentage. Similar pattern can be identified for

velocity distribution as illustrated in Figure-9. The velocity is relatively higher at 20% of filling than at the rest of filling percentage.

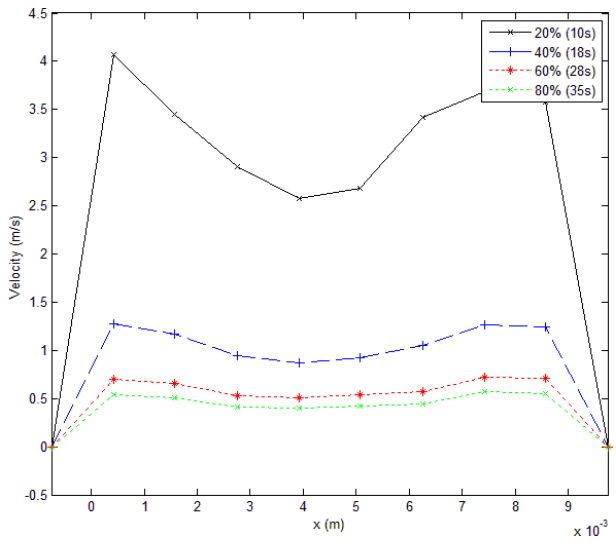

Figure-9. Velocity distribution near inlet at different filling percentage of PUF encapsulation.

Even though pressure and velocity effect shows declining trend over time, they both possess a relatively high value at the onset of the filling. It was notable that PUF can lead to a much faster encapsulation, however, it is crucial to take caution on the after effect of pressure and velocity on the reliability of BGA package manufactured.

CONCLUSIONS

This paper studies the effect of pressurized flow on the filling time, pressure and velocity distribution throughout the pressurized filling process. At the start of the filling, highest pressure distribution can be observed with value near to 344MPa due to continuous pressurized flow at the inlet dispenser. This value however slowly depreciates as the flow hit more solder bumps. Considerable delay can be seen for 80% filling percentage with only 70% space occupied. As a result, racing effect phenomena occurs and could result to incomplete filling and voids formation. Therefore, the pressurized flow needs to be controlled to reduce the amount of unoccupied spaces during flow propagation. Increasing the number of inlet dispensers could also prove viable to reduce the racing effect problem.

ACKNOWLEDGEMENT

The work was partly supported by the Short Term Grant 60313020 by UniversitiSains Malaysia, Engineering Campus, Penang.

REFERENCES

[1] C. Y. Khor, M. Abdul Mujeebu, M. Z. Abdullah, and F. Che Ani. 2010. Finite volume based CFD simulation of pressurized flip-chip underfill encapsulation process. Microelectron. Reliab. vol. 50, no. 1, pp. 98-105.

[2] Chih-Chung Hsu, Hsien-Sen Chiu, and Rong-Yeu Chang. 2012. 3D simulation of underfill encapsulation in semiconductor processing. 7th International Microsystems, Packaging, Assembly and Circuits Technology Conference (IMPACT). pp. 224-227.

[3] H. Ardebili and M. G. Pecht. 2009. Encapsulation Technologies for Electronic Applications. Elsevier, pp. 129-179.

[4] H. Gwon, H. Lee, J.-M. Kim, Y. Shin, and S. Lee. 2014. Dynamic behavior of capillary-driven encapsulation flow characteristics for different injection types in flip chip packaging. J. Mech. Sci. Technol. vol. 28, no. 1, pp. 167-173.

[5] H. Wang, H. Zhou, Y. Zhang, D. Li, and K. Xu. 2011. Three-dimensional simulation of underfill process in flip-chip encapsulation. Comput. Fluids. vol. 44, no. 1, pp. 187-201.

[6] K. M. Chen. 2008, Comparing the Impacts of the Capillary and the Molded Underfill Process on the Reliability of the Flip-Chip BGA. Components and Packaging Technologies, IEEE Transactions on, vol. 31, no. 3. pp. 586-591.

[7] M. K. Abdullah, M. Z. Abdullah, M. A. Mujeebu, S. Kamaruddin, and Z. M. Ariff. 2009. A Study on the Effect of Epoxy Molding Compound (EMC) Rheology during Encapsulation of Stacked-CHIP Scale Packages (S-CSP). J. Reinf. Plast. Compos. vol. 28, no. 20, pp. 2527-2538.

[8] R.-Y. Chang, W.-H. Yang, S.-J. Hwang and F. Su. 2004. Three-Dimensional Modeling of Mold Filling in Microelectronics Encapsulation Process. IEEE Trans. Components Packag. Technol. vol. 27, no. 1, pp. 200-209.

[9] R. Chang and W. Yang. 2001. Numerical simulation of mold filling in injection molding using a three-dimensional finite volume approach. Int. J. Numer. Methods Fluids. vol. 37, no. 2, pp. 125-148.

[10] R. Han, L. Shi, and M. Gupta. 2000. Three-dimensional simulation of microchip encapsulation process. Polym. Eng. Sci. vol. 40, no. 3, pp. 776-785.

[11] R.-Y. Chang, W.-H. Yang, S.-J. Hwang and F. Su. 2004. Three-Dimensional Modeling of Mold Filling in Microelectronics Encapsulation Process. IEEE Trans. Components Packag. Technol. vol. 27, no. 1, pp. 200-209.

[12] T. Hashimoto, T. Shin-ichiro, K. Morinishi, and N. Satofuka. 2008. Numerical simulation of conventional capillary flow and no-flow underfill in flip-chip packaging. Comput. Fluids. vol. 37, no. 5, pp. 520-523.